
**Separation Science and Technology**
Publication details, including instructions for authors and subscription information:
http://www.informaworld.com/smpp/title~content=t713708471

# Optimum Design of a Solid-Liquid Stirred System by Taking into Account the Propagation of Turbulent Energy

Michio Nonaka[a]
[a] DEPARTMENT OF MINERAL DEVELOPMENT ENGINEERING, THE UNIVERSITY OF TOKYO, TOKYO, JAPAN

**To cite this Article** Nonaka, Michio(1990) 'Optimum Design of a Solid-Liquid Stirred System by Taking into Account the Propagation of Turbulent Energy', Separation Science and Technology, 25: 6, 753 — 779
**To link to this Article: DOI:** 10.1080/01496399008050364
**URL:** http://dx.doi.org/10.1080/01496399008050364

SEPARATION SCIENCE AND TECHNOLOGY, 25(6), pp. 753-779, 1990

# Optimum Design of a Solid-Liquid Stirred System by Taking into Account the Propagation of Turbulent Energy

MICHIO NONAKA

DEPARTMENT OF MINERAL DEVELOPMENT ENGINEERING
THE UNIVERSITY OF TOKYO
TOKYO 113, JAPAN



**Abstract**

The mixing behavior of material in a stirred vessel is generally governed by macromixing due to circulating convective flow and micromixing due to turbulent fluctuating flow. The mixing energy is consumed more in micromixing than in macromixing, and hence the propagation of turbulent energy has to be evaluated explicity for the optimum design and scale-up formulation. The energy spectrum function of turbulence in a stirred vessel was derived from the Eulerian time correlation function of fluctuation velocities, and then the decay of turbulent energy was evaluated by the spectrum function. The stochastic mean of the fluctuating velocities, the integral space scale of turbulence, and the energy dissipation rate were correlated with the operating variables of the stirred vessel, and the spatial distributions of these characteristics were calculated in the macromixing and/or micromixing flow fields. Particle behavior in a solid-liquid two-phase system was numerically analyzed by using an axial diffusion equation with a space variant diffusion coefficient. Finally, as a mass transfer model the turbulent diffusive coagulation of fine particles was evaluated in reference to the optimum design of the stirred vessel.

## INTRODUCTION

The mixing behavior of materials in a stirred vessel is generally governed by macromixing due to circulating convective flow and micromixing due to turbulent fluctuating flow. The effect of turbulent mic-

romixing on the mixing characteristics with or without the presence of simple mass transfer or complex chemical reaction has to be evaluated explicitly because more mixing energy is consumed in micromixing than in macromixing. Turbulent energy supplied to the stirred medium through the rotation of the impeller is propagated convectively and diffusively into all spaces in the vessel. In the meantime, the kinematic energy of the observed fluid element is dissipated by the viscosity effect. Thus, it is essential to take into account the decay process of turbulent energy for the optimum design and scale-up formulation of a stirred system.

Macromixing characteristics have hitherto been studied mostly in terms of the operating variables as well as of the geometric dimensions of the stirred vessels (*1–5*). Many types of scale-up formulas have also been derived from these considerations. These formulas have not, however, been unified, and hence it is very difficult to decide which is the most suitable scale-up formula. Some recent approaches incorporate turbulent characterisitcs in the optimum design or scale-up formulation of stirred vessels (*6–10*). The dissipation rate of turbulent energy is regarded as one of the most effective factors in the design of stirred vessels. The dissipation rate is determined by the stochastic mean of the fluctuating velocities, the space scale of turbulence, and the kinematic viscosity of the stirred medium. These characteristics are spatially distributed, and hence it is impossible to draw a precise picture of the mixing phenomenon in a stirred vessel when only the overall characteristics are taken into account.

In this article the energy spectrum function is identified from the Eulerian time correlation function of fluctuating velocities, and then the decay process of the supplied turbulent energy is evaluated. The effects of operating variables on particle behavior in solid–liquid two-phase systems are numerically analyzed by using an axial diffusion equation with a space variant diffusion coefficient. Finally, as a mass transfer model, the turbulent diffusive coagulation of fine particles is evaluated in reference to the optimum design of a stirred vessel.



## ENERGY SPECTRUM FUNCTION IN A STIRRED VESSEL

When the inertia and pressure gradient terms in the Navier-Stokes equation are disregarded, the fluctuating velocity of a fluid element in a stirred vessel is described by

$$\frac{\partial u(x,t)}{\partial t} = \nu \frac{\partial^2 u(x,t)}{\partial x^2} \tag{1}$$

where $u$ denotes the fluctuating velocity, $\nu$ is the kinematic viscosity of the stirred medium, and $x$ and $t$ are space and time coordinates, respectively. When $u(x,t) = 0$ at $t > 0$ and $x = \infty$, Eq. (1) is solved analytically and

$$u(x,t) = (4\pi\nu t)^{-1/2} \exp\left(-\frac{x^2}{4\nu t}\right) \tag{2}$$

is obtained. Hence, the longitudinal velocity correlation function between two points on the trajectory of an observed turbulent eddy is given by

$$f(r,t) = \frac{\int_0^\infty u(x,t)u(x+r,t)dx}{\int_0^\infty u^2(x,t)dx} = \exp\left(-\frac{r^2}{8\nu t}\right) \tag{3}$$

where $r$ denotes the distance between two points.

Assuming that mass transfer is caused by the fluctuating velocity, Eq. (1) can represent the microprocess of mass transfer in a stirred vessel in which turbulent energy is propagated by diffusive mixing. It has been generally confirmed that the velocity correlation functions observed in Lagrangian and Eulerian coordinate systems are consistent with each other in their functional forms (*11*). By substituting

$$\Lambda_f = \sqrt{2\pi\nu t} \tag{4}$$

$$r = U \cdot \tau \tag{5}$$

$$T_E = \frac{\Lambda_f}{U} \tag{6}$$

for Eq. (3) the Eulerian time correlation function is written as

$$R_E(\tau) = \exp\left(-\frac{\pi\tau^2}{4T_E^2}\right) \tag{7}$$

where $\tau$ denotes the time increment, $U$ is the mean velocity, and $T_E$ is the integral time scale of turbulence defined by

$$T_E = \int_0^\infty R_E(\tau)d\tau \tag{8}$$

Equation (7) has been verified through the time series analysis for observed fluctuating velocities (*12*).

By substituting Eq. (4) for Eq. (3), the longitudinal velocity correlation function is rewritten as

$$f(r) = \exp\left(-\frac{\pi r^2}{4\Lambda_f^2}\right) \tag{9}$$

$$\Lambda_f = \int_0^\infty f(r)dr \tag{10}$$

and the energy spectrum function in isotropic turbulence is given by

$$E(\kappa) = \frac{4\overline{u^2}}{\pi^3}\ \Lambda_f^5\kappa^4 \exp\left(-\frac{\Lambda_f^2\kappa^2}{\pi}\right) \tag{11}$$

where $\Lambda_f$ denotes the integral space scale of turbulence and $\kappa$ denotes the wavenumber. Hence, overall turbulent energy is given by

$$\int_0^\infty E(\kappa)d\kappa = \frac{3}{2}\overline{u^2} \tag{12}$$

The energy transfer process in isotropic turbulence is described by

$$\frac{\partial E(\kappa,t)}{\partial t} = T(\kappa,t) - 2\nu\kappa^2 E(\kappa,t) \tag{13}$$

where $T(\kappa,t)$ denotes the energy transfer function. Equation (13) means that the variation of energy contained in eddies of wavenumber $\kappa$ per unit time is given by the difference between incoming energy due to inertia and dissipating enrgy due to viscosity. Assuming that the energy transfer function can be disregarded, the energy spectrum function is written as

$$E(\kappa,t) = E(\kappa,0) \exp(-2\nu\kappa^2 t) \tag{14}$$

where $E(\kappa,0)$ is the initial energy spectrum function which can be given by

$$E(\kappa,0) = \gamma\kappa^4 \tag{15}$$

taking into account the functional form of Eq. (11). Consequently, the energy spectrum function for turbulence in a stirred vessel is represented by

$$E(\kappa,t) = \gamma\kappa^4 \exp(-2\nu\kappa^2 t) \tag{16}$$

## DECAY PROCESS OF TURBULENT ENERGY

By substituting Eq. (16) for Eq. (12), the decay of turbulent energy supplied at a source of turbulence is described by

$$\overline{u^2} = \sqrt{\pi}\ \frac{\gamma}{4}(2\nu t)^{-5/2} \tag{17}$$



The integral space scale is varied with time according to Eq. (4). Equations (17) and (4) cannot, however, be defined at $t \to 0$. To cope with this problem the following procedures can be introduced, and then Eqs. (17) and (4) will be transformed into practical, useful formulas.

The first procedure is based on the idea that the stochastic mean of the fluctuating velocities is observed as $\sqrt{\overline{u_m^2}}$ in the vicinity of the impeller. It is propagated into the bulk of the stirred medium with a velocity of $\sqrt{\overline{u^2}}$. Thus the transport length from the observed point is given by

$$L = \int_{t_0}^{t} \sqrt{\overline{u^2}}\, dt \tag{18}$$

Hence, Eqs. (17) and (4) are rewritten as

$$\overline{u^2} = \sqrt{\pi}\ \frac{\gamma}{4}(2\nu)^{-5/2}\left[t_0^{-1/4} - \left(\frac{2\nu^5}{\pi\gamma^2}\right)^{1/4} L\right]^{10} \tag{19}$$

$$\Lambda_f = (2\pi\nu)^{1/2}\left(t_0^{-1/4} - \left(\frac{2\nu^5}{\pi\gamma^2}\right)^{1/4} L\right]^{-2} \tag{20}$$

where $t_0$ and $\gamma$ are determined by

$$t_0 = \frac{1}{2\nu}\left(\frac{4\overline{u_m^2}}{\sqrt{\pi}\gamma}\right)^{-2/5} \tag{21}$$

$$\gamma = \frac{4}{\pi^3} \overline{u_m^2} \Lambda_{f,m}^5 \tag{22}$$

Equation (19) has been verified through a series of experiments carried out using a stirred vessel without convective flow (*12*).

The second procedure includes the convective transport of turbulent energy specified by the discharge flow from the impeller. It is assumed that the mean velocity of the discharge flow is given by

$$w = w_0 \exp(-\alpha L) \tag{23}$$

where $w_0$ is the initial flow velocity observed in the vicinity of the impeller and $\alpha$ is the coefficient determined by the mixing characteristics of the impeller. The initial velocity is given by

$$w_0 = \frac{8N_f}{\pi} nd\left(\frac{d}{D}\right)^2 \tag{24}$$

where $n$ is the rotational speed of the impeller, $d$ is the diameter of the impeller, $D$ is the diameter of the cylindrical vessel, and $N_f$ is the flow number of the impeller (*3*). The flow number is defined by

$$N_f = \frac{Q}{nd^3} \tag{25}$$

where $Q$ denotes the volume flow rate of the discharge flow. The relationship between the transport time $t$ and the transport length $L$ is derived from the integration of Eq. (23), which is represented by

$$t = \frac{1}{\alpha w_0}\{\exp(\alpha L) - 1\} \tag{26}$$

Hence the turbulent energy and the integral space scale given by

$$\overline{u^2} = \sqrt{\pi}\ \frac{\gamma}{4}(2\nu)^{-5/2}(t + t_0)^{-5/2} \tag{27}$$

and

$$\Lambda_f = \sqrt{2\pi\nu(t + t_0)} \tag{28}$$

can be rewritten as the function of the transport length, respectively.

Effects of the operating variables of the stirred vessel on the turbulent characteristics have to be quantified for the optimum design. It can be easily inferred that the energy dissipation rate and the stochastic mean of the fluctuating velocities observed in the vicinity of the impeller are given by

$$\varepsilon_m = a_1 n^3 d^2 \left(\frac{d}{D}\right)^3 \tag{29}$$

$$\sqrt{\overline{u^2}_m} = a_3 n d \left(\frac{d}{D}\right) \tag{30}$$

respectively, where $a_1$ and $a_3$ are proportional constants. Moreover, the energy dissipation rate is correlated with the mean fluctuating velocity and the space scale in the case where turbulence in the vicinity of the impeller is isotropic, which is given by

$$\varepsilon_m = -2\nu \int_0^\infty \kappa^2 E(\kappa,t) d\kappa$$

$$= \frac{15\pi\nu\overline{u^2}_m}{2\Lambda_{f,m}^2} \tag{31}$$

Hence, the observed space scale is written as

$$\Lambda_{f,m} = \alpha_2 \sqrt{\left(\frac{\nu}{n}\right)\left(\frac{D}{d}\right)} \tag{32}$$

where $a_2$ is the proportional constant determined by

$$a_2 = \frac{15\pi {a_3}^2}{2a_1} \tag{33}$$

The turbulent diffusion coefficient is defined by

$$D_t = \eta \sqrt{\overline{u^2}} \Lambda_f \tag{34}$$

where $\eta$ is the coefficient determined by the relationship between Lagrangian and Eulerian turbulent characteristics, which has been recog-

nized as 0.4 in homogeneous turbulence (*11*). Consequently, we can determine the distribution of the turbulent diffusion coefficients in the axial direction in the stirred vessel by using Eqs. (19) and (20) in the case where turbulent energy is propagated by turbulent diffusion only, or by using Eqs. (27) and (28) in the case where turbulent energy is transported with convective flow.

## FORMULATION OF PARTICLE BEHAVIOR IN A STIRRED VESSEL

The behavior of solid particles in the axial direction in a solid-liquid stirred system is described by

$$\frac{\partial C}{\partial t} = \frac{\partial (vC)}{\partial z} + \frac{\partial}{\partial z}\left(D_t' \frac{\partial C}{\partial z}\right) \tag{35}$$

where $C$ denotes the solids concentration on a count basis, $v$ is the particle velocity in the $z$-direction, $D_t'$ is the turbulent diffusion coefficent of solid particles, and $z$ is the axial space coordinate with its origin on the bottom of the stirred vessel. The turbulent diffusion coefficient is derived from analyzing for the turbulent motion of solid particles. The ratio of the fluctuation spectrum for a particle to that for a fluid element in an isotropic turbulent field is given by

$$\frac{\mathrm{Su}_p}{\mathrm{Su}_f} = \frac{A^2 + B^2\omega^2}{A^2 + \omega^2} \tag{36}$$

where $\mathrm{Su}_p$ and $\mathrm{Su}_f$ are the spectrum densities for particle and fluid fluctuating motions, respectively, and $\omega$ is the frequency (*13*). $A$ and $B$ are defined by

$$A = \frac{36\mu_f}{(2\rho_p + \rho_f)d_p^2} \tag{37}$$

$$B = \frac{3\rho_f}{2\rho_p + \rho_f} \tag{38}$$

where $d_p$ is the particle diameter, $\rho_p$ and $\rho_f$ are the particle and fluid densities, respectively, and $\mu_f$ is the fluid viscosity Equation (36) is illustrated in Fig. 1. The frequency of the turbulent fluctuation may generally be

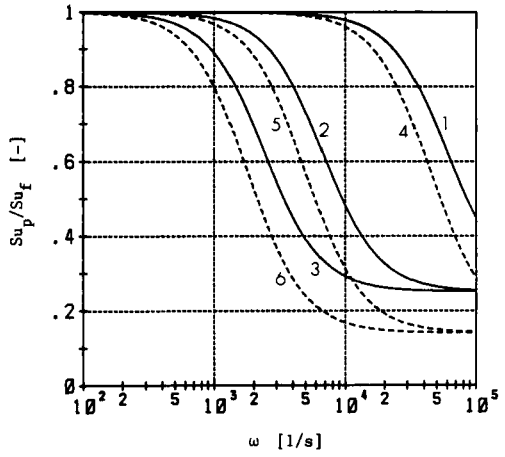


FIG. 1. Relative spectrum density of the particle fluctuation in turbulence. Fluid density $\rho_f$ = 1000 kg/m$^3$, fluid viscosity $\mu_f$ = 1 mPa · s. Particle density $\rho_p$ (kg/m$^3$), particle diameter $d_p$ (μm): (1) $\rho_p$ = 2500, $d_p$ = 10; (2) $\rho_p$ = 2500, $d_p$ = 30; (3) $\rho_p$ = 2500, $d_p$ = 50; (4) $\rho_p$ = 3500, $d_p$ = 10; (5) $\rho_p$ = 3500, $d_p$ = 30; (6) $\rho_p$ = 3500, $d_p$ = 50.



below $10^3$ s$^{-1}$ in practical stirred vessels and, hence, it can be assumed that a solid particle smaller than a few tens of a μm moves along with the surrounding fluid elements. Therefore, it might by hypothesized that $D_t'$ involved in Eq. (35) can be replaced by Eq. (34). Although Eq. (36) is derived from disregarding the effect of the Basset historical term on the particle motion, this hypothesis has also been proved to be reasonable in the case where the Basset term is taken into account (*14*).

The coagulation process due to mutual collisions of fine particles in a turbulent field is discussed as a model of mass transfer processes to evaluate the optimum design of the solid-liquid stirred system. The turbulent coagulation rate on a count basis per unit volume of the stirred medium is accepted as a performance index, which is given by

$$N_c = K\pi\beta\sqrt{\frac{\varepsilon}{\nu}d_p^3C^2} \tag{39}$$

where the particle size is smaller than the Kolmogorov's microscale of turbulence (*15*). The coefficient $K$ involved in Eq. (39) should be 24 when par-

ticles coming into collisions move independently, while $K$ should be 12 when the particle motion is mutually dependent. In the following calculations, $K$ will be fixed to 12, and 1/15 will be substituted for another coefficient $\beta$.

## NUMERICAL ANALYSIS

A stirred vessel of the open top type and with a cylindrical configuration is analyzed for optimum design. The diameter $D$ is 0.3 m and the height $H$ is 0.3 m. A monodispersed system composed of particles with a diameter of 30 μm and a polydispersed system containing particles of 10, 20, 30, and 50 μm are evaluated. The particle density is fixed to 2500 kg/m$^3$. It has been confirmed that these particles are smaller than the Kolmogorov's microscale of turbulence in the stirred vessel. In the following calculations the axial distributions of the energy dissipation rate and the solids concentration will be numerically analyzed for steady batch processes with or without convective flow at first, and then the turbulent coagulation rate will be pursued. The coagulation rate is evaluated by the mean particle size on a count basis in the polydispersed system. The energy loss by friction on the side wall or on the bottom of the vessel is not taken into account. Moreover, the effect of the distribution of the solids concentration on the energy propagation process is disregarded in this analysis.

The following conditions are selected as the standard criteria: the location of the impeller $z_0$ is 0.15 m, the rotational speed of the impeller $n$ is 3 s$^{-1}$, the diameter of the impeller $d$ is 0.15 m, the coefficients $a_2$ and $a_3$ involved in Eqs. (32) and (30) are 3 and 0.5, respectively, and the mean solids concentration on a volume basis is 0.01. The mixing Reynolds number is defined by

$$N_{\mathrm{Re}} = \frac{nd^2}{\nu} \tag{40}$$

and is 67,500. Hence, the flow in the stirred vesel is turbulent. The concentration profiles in the axial direction for solid particles with diameters of 10, 20, 30, 40, and 50 μm, respectively, are shown in Fig. 2, in which the solids concentrations is normalized by the mean concentration. These numerical results have been verified through a series of experiments carried out by using sharply classified glass beads.

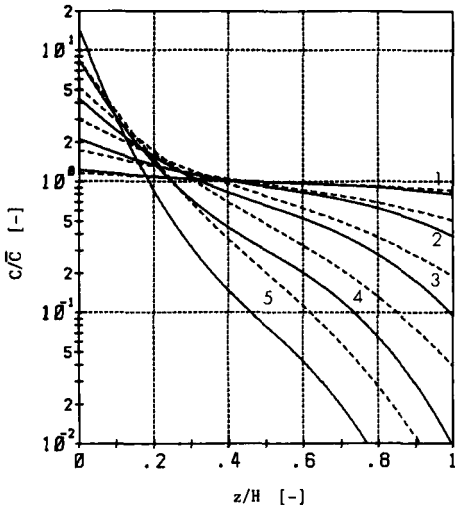


FIG. 2. Distribution of the solids concentration of particles with various sizes. Solid lines correspond to turbulent diffusion only, while broken lines correspond to turbulent diffusion with convection. $z_0 = 0.15$ m, $n = 3\ s^{-1}$, $d = 0.15$ m. Particle diameter $d_p$ (μm): (1) 10, (2) 20, (3) 30, (4) 40, (5) 50.



The effect of impeller size on the concentration profile for monodispersed particles and the distribution of the energy dissipation rate are shown in Figs. 3 and 4, respectively. The local energy dissipation rate is also normalized by the overall dissipation rate. The coefficients α and $N_f$ involved in Eqs. (23) and (24) are 0.8 and 10, respectively. As can be seen, the larger the impeller size, the more uniformly the concentration and the dissipation energy are distributed. The relationship between the overall dissipation energy, called the specific agitation energy $\bar{\varepsilon}$, and the overall coagulation rate, $\bar{N}_c$, is introduced to evaluate the effect of the impeller size on the coagulation process in the case where the location of the impeller is varied, which appears in Fig. 5. As can be seen, the overall coagulation rate increases with the increase of the specific agitation energy caused by the increase of the impeller size, and the coagulation rate also becomes faster as the location of the impeller becomes lower.

The effect of the rotational speed of the impeller on the coagulation rate is shown in Fig. 6. The overall coagulation rate increases with the increase

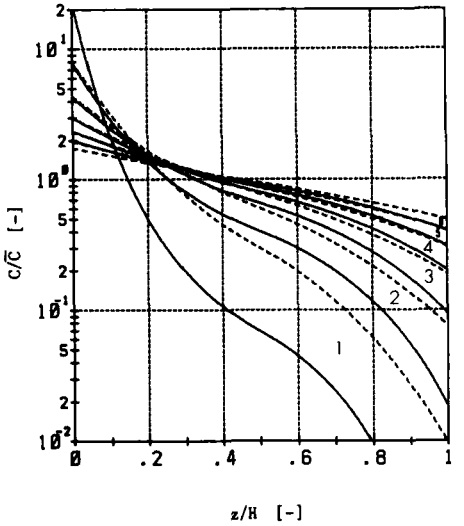


FIG. 3. Effect of the impeller size on the solids concentration profile. Solid lines correspond to turbulent diffusion only, while broken lines correspond to turbulent diffusion with convection. $d_p = 30$ μm, $n = 3\ s^{-1}$, $z_0 = 0.15$ m. Impeller diameter $d$ (m): (1) 0.1, (2) 0.125, (3) 0.15, (4) 0.175, (5) 0.2, (6) 0.225.



of the specific agitation energy caused by the increase of the rotational speed of the impeller. A faster coagulation rate is observed when the impeller is located at a lower position. Thus, it is concluded that coagulation performance is improved when the larger impeller is located at the lower position in the stirred vessel.

The effect of the location of the impeller on the coagulation rate has been analyzed for monodispersed and polydispersed systems. Some of the results are shown in Fig. 7. As can be seen, the turbulent coagulation performance in the stirred vessel is significantly affected by the location of the source of turbulence. Similar numerical results have been obtained under different rotational speeds and different impeller sizes. The distributions of the solids concentration, the dissipation rate of turbulent energy, and the local coagulation rate are strongly affected by the location of the impeller. The numerical results are shown in Figs. 8, 9, and 10. The concentration profiles show that particles existing in the upper region tend to settle into the lower space when the impeller is located at the lower position, while particles in the lower space of the vessel settle more easily in the case where the impeller is located at the upper position of the vessel.

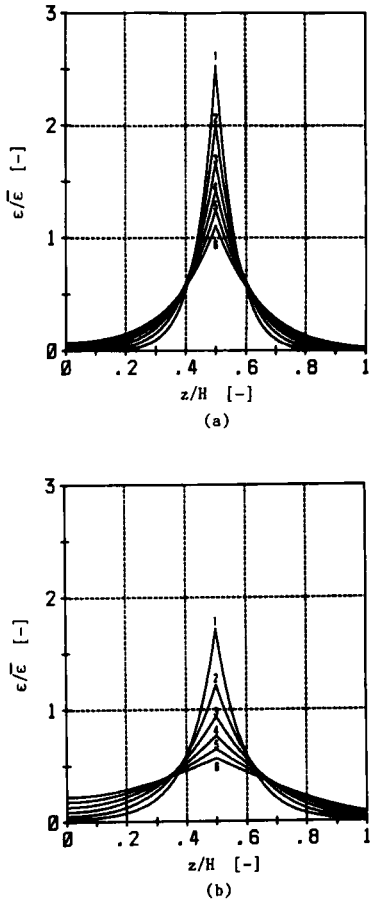


FIG. 4. Effect of the impeller size on the distribution of the dissipation energy. (a) Turbulent diffusion only, (b) turbulent diffusion with convection. $z_0$ = 0.15 m, $n$ = 3 $s^{-1}$. Impeller diameter $d$ (m): (1) 0.1, (2) 0.125, (3) 0.15, (4) 0.175, (5) 0.2, (6) 0.225.

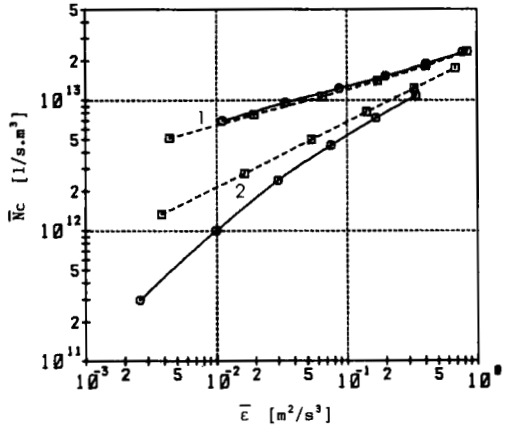


FIG. 5. Dependence of the overall coagulation rate on the specific agitation energy in the case where the impeller size is varied. Solid lines correspond to turbulent diffusion only, while broken lines correspond to turbulent diffusion with convection. $d_p$ = 30 μm, $n$ = 3 s$^{-1}$; (1) $z_0$ = 0.05 m, (2) $z_0$ = 0.15 m.



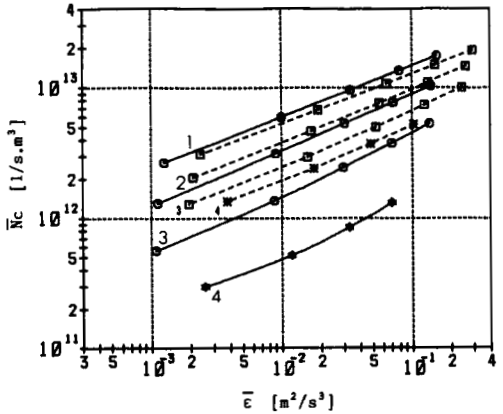


FIG. 6. Dependence of the overall coagulation rate of monodispersed particles on the specific agitation energy in the case where the rotational speed of the impeller is varied. Solid lines correspond to turbulent diffusion only, while broken lines correspond to turbulent diffusion with convection. (1) $z_0$ = 0.05 m, $d$ = 0.15 m; (2) $z_0$ = 0.1 m, $d$ = 0.15 m; (3) $z_0$ = 0.15 m, $d$ = 0.15 m; (4) $z_0$ = 0.15 m, $d$ = 0.1 m.

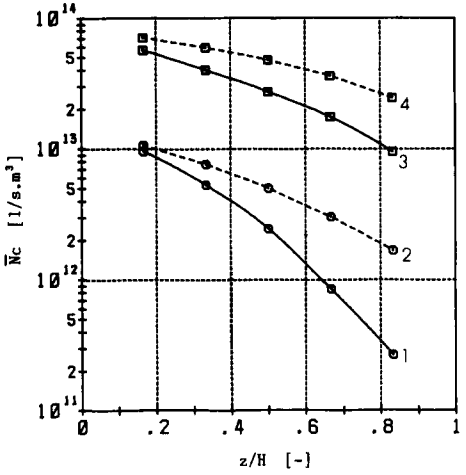


FIG. 7. Effect of the location of the impeller on the overall coagulation rate in the monodispersed and polydispersed systems. $n = 3\ s^{-1}$, $d = 0.15$ m. (1) Monodispersed, turbulent diffusion only; (2) monodispersed, turbulent diffusion with convection; (3) polydispersed, turbulent diffusion only; (4) polydispersed, turbulent diffusion with convection.



Moreover, it can be seen from Fig. 8 that turbulent energy is more uniformly propagated by an impeller located at the lower position than by an impeller located at the upper position. As a result, the local coagulation rate is distributed as shown in Fig. 10. Moreover, it has been found that the specific agitation energy is approximately constant even when the location of the impeller is varied.

There are many operations in which multiple impellers have to be used; for instance, to make the solids concentrtion severely uniform with slow rotational speeds of the impellers. The concentration profiles have been analyzed for a stirred system with two-stage impellers by varying each rotational speed and keeping the sum of the speeds constant, which appear in Fig. 11. As can be seen, the profiles vary regularly by changing the combination of rotational speeds in the case where the locations and the diameters of the impellers are kept constant. The distributions of the energy dissipation rate and the space scale of turbulence, which is written as the ratio of the integral scale to Kolmogorov's microscale of turbulence $\lambda_0$, are shown in Figs. 12 and 13. It can also be seen that these profiles show approximately symmetrical patterns. The effects of the specific agitation energy on the coagulation rates of monodispersed and polydispersed par-

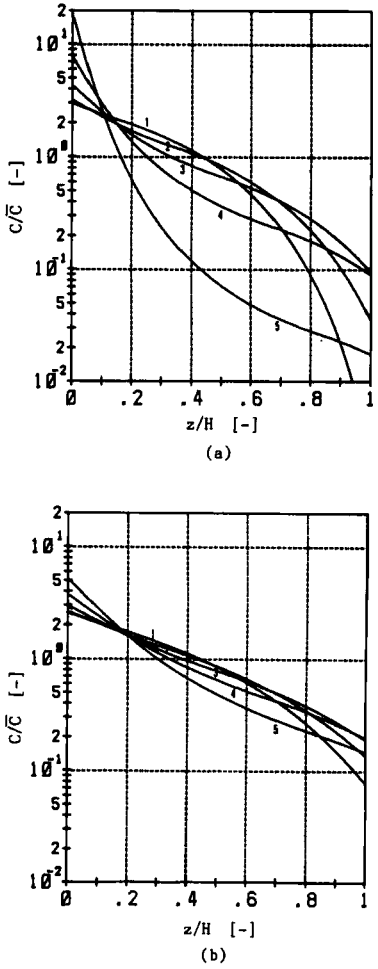


FIG. 8. Effect of the location of the impeller on the solids concentration profile for monodispersed particles. (a) Turbulent diffusion only, (b) turbulent diffusion with convection, $n = 3$ $s^{-1}$, $d = 0.15$ m. Location of the impeller $z_0$ (m): (1) 0.05, (2) 0.1, (3) 0.15, (4) 0.2, (5) 0.25.

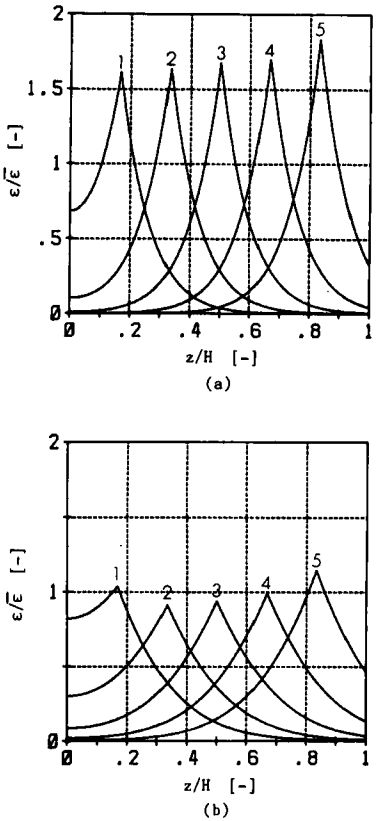


FIG. 9. Effect of the location of the impeller on the distribution of the dissipation energy. (a) Turbulent diffusion only (b) turbulent diffusion with convection, $n = 3\ s^{-1}$, $d = 0.15$ m. Location of the impeller $z_0$ (m): (1) 0.05, (2) 0.1, (3) 0.15, (4) 0.2, (5) 0.25.

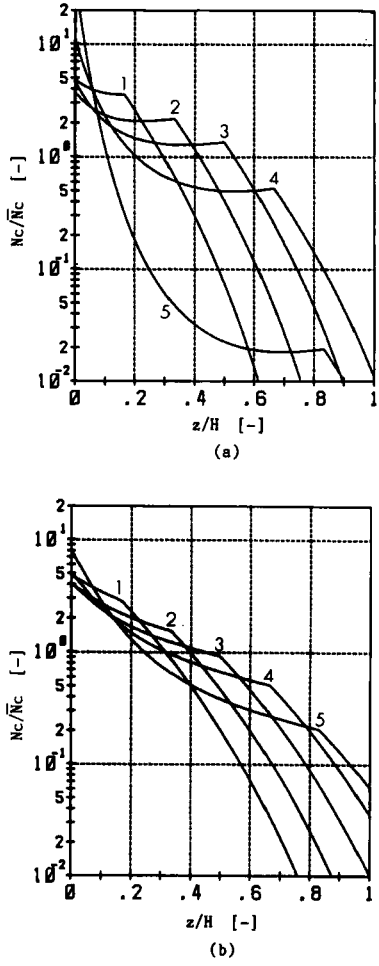


FIG. 10. Effect of the location of the impeller on the distribution of the coagulation rate of monodispersed particles. (a) Turbulent diffusion only (b) turbulent diffusion with convection. $n = 3\ s^{-1}$, $d = 0.15$ m. Location of the impeller $z_0$ (m): (1) 0.05, (2) 0.1, (3) 0.15, (4) 0.2, (5) 0.25.

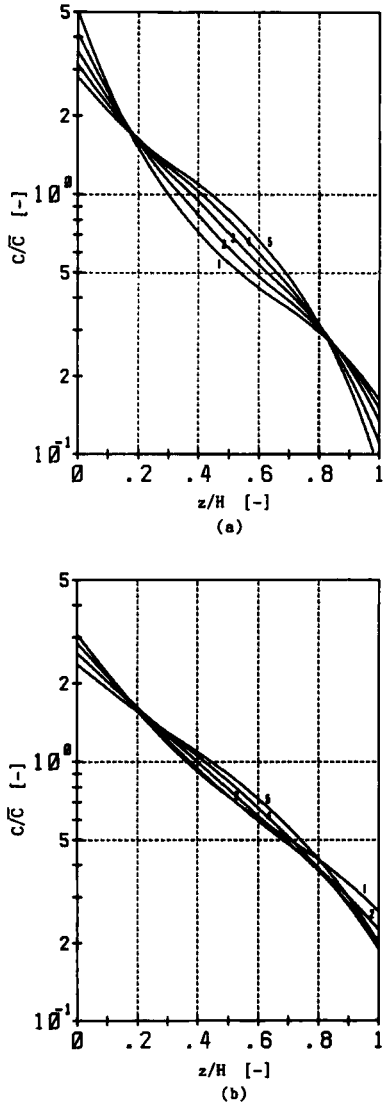


FIG. 11. Solids concentration profiles of monodispersed particles in the stirred vessel with two-state impellers operated under various rotational speeds. (a) Turbulent diffusion only, (b) turbulent diffusion with convection. $z_0$ = (0.1, 0.2) m, $d$ = (0.15, 0.15) m. Rotational speeds of the impellers $n$ ($s^{-1}$): (1) (0.5, 0.25); (2) (1, 2); (3) (1.5, 1.5); (4) (2, 1); (5) (2.5, 0.5).

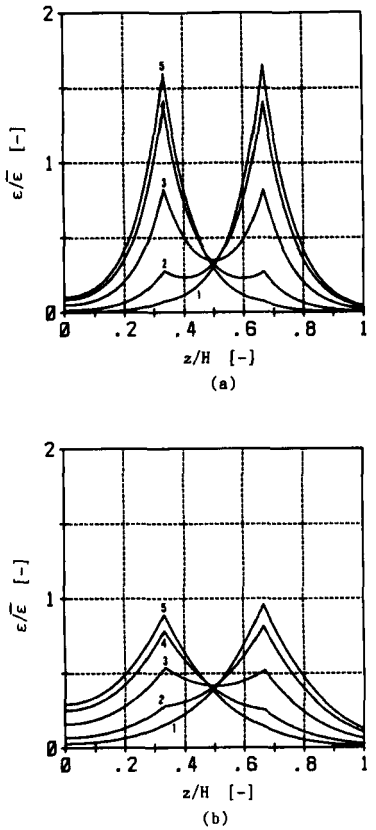


FIG. 12. Distribution of the dissipation energy in the stirred vessel with two-stage impellers operated under various rotational speeds. (a) Turbulent diffusion only, (b) turbulent diffusion with convection. $z_0$ = (0.1, 0.2) m; $d$ = (0.15, 0.15) m. Rotational speeds of the impellers $n$ ($s^{-1}$): (1) (0.5, 2.5); (2) (1, 2); (3) (1.5, 1.5); (4) (2, 1); (5) (2.5, 0.5).

ticles are illustrated in Fig. 14. Thus, it is revealed that a faster coagulation rate can be obtained by selecting a combination of appropriate rotational speeds that keeps the specific agitation energy constant.

Another numerical analysis has been done for a stirred vessel with two-stage impellers located at various positions. The diameters and rotational speeds of the impellers have been kept constant. One of the impellers was located at a fixed position, while the position of the other impeller was varied. The coagulation performance is shown in Fig. 15. It is found that

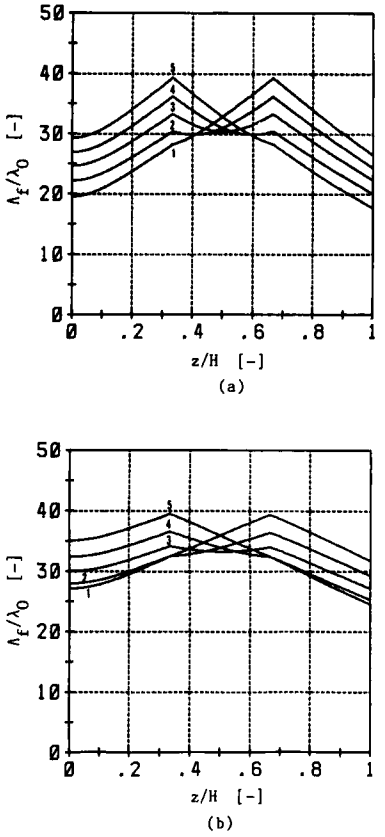


FIG. 13. Distribution of the integral space scale in the stirred vessel with two-stage impellers operated under various rotational speeds. (a) Turbulent diffusion only, (b) turbulent diffusion with convection. $z$ = (0.1, 0.2) m; $d$ = (0.15, 0.15) m. Rotational speeds of the impeller $n$ ($s^{-1}$): (1) (0.5, 2.5); (2) (1, 2); (3) (1.5, 1.5); (4) (2, 1); (5) (2.5, 0.5).

the specific agitation energy is not alterated much, but the overall coagulation rate is drastically varied.

Moreover, the effect of the number of multiple impellers on the coagulation performance was numerically analyzed for the monodispersed system. The relationship between the specific agitation energy and the overall coagulation rate is shown in Fig. 16 where the peripheral speed of each impeller is kept constant. This constraint has been accepted sometimes as an empirical scale-up rule. It can be seen from Fig. 16, however, that the rule is not as reasonable as for the turbulent coagulation process.

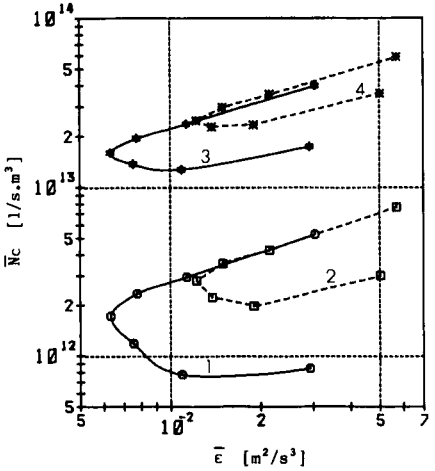


FIG. 14. Dependence of the overall coagulation rate on the specific agitation energy of the stirred vessel with two-stage impellers operated under various rotational speeds. Sum of the rotational speeds is fixed to 3 $s^{-1}$. $z_0$ = (0.1, 0.2) m; $d$ = (0.15, 0.15) m. (1) Monodispersed, turbulent diffusion only; (2) monodispersed, turbulent diffusion with convection; (3) polydispersed, turbulent diffusion only; (4) polydispersed, turbulent diffusion with convection.

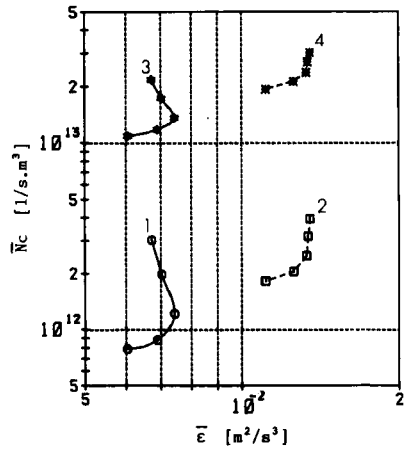


FIG. 15. Dependence of the overall coagulation rate on the specific agitation energy of the stirred vessel with two-stage impellers located at various positions. One of the impellers is located at the fixed position $z_0$ = 0.15 m, while the location of the other is varied. (1) Monodispersed, turbulent diffusion only; (2) monodispersed, turbulent diffusion with convection; (3) polydispersed, turbulent diffusion only; (4) polydispersed, turbulent diffusion with convection.

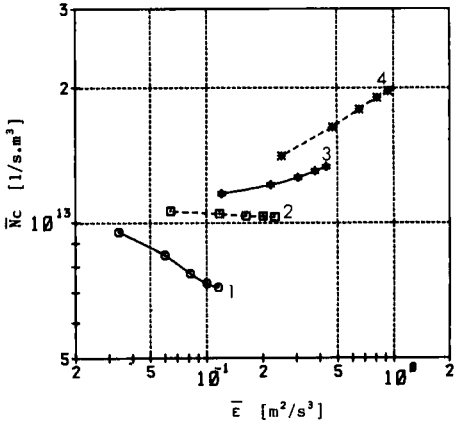


FIG. 16. Dependence of the overall coagulation rate of monodispersed particles on the specific agitation energy in the stirred vessel with multiple impellers. The specific agitation energy energy is varied by the number of impellers located at $z_0$ = (0.05, 0.1, 0.15, 0.2, 0.25), (0.05, 0.1, 0.15, 0.2), (0.05, 0.1, 0.15), (0.05, 0.1), and (0.05) m. (1) $n$ = 3 s$^{-1}$, $d$ = 0.15 m, turbulent diffusion only; (2) $n$ = 3 s$^{-1}$, $d$ = 0.15 m, turbulent diffusion with convection; (3) $n$ = 2 s$^{-1}$, $d$ = 0.225 m, turbulent diffusion only; (4) $n$ = 2 s$^{-1}$, $d$ = 0.225 m, turbulent diffusion with convection.



It is also found that there is an operating condition under which multiple impellers cause a decrease of the coagulation rate in spite of an increase of the agitation power. Consequently, the number of impellers has to be selected according to the objective of the mixing process.

The effects of the constants $a_2$ and $a_3$ involved in Eqs. (32) and (30), respectively, on the coagulation performance have been numerically analyzed to pursue the optimum impeller-baffle plate structure. The coagulation performance is shown in Fig. 17 for the case where the mean fluctuating velocity or the integral space scale of turbulence in the vicinity of the impeller is varied by changing the respective constants. As can be seen, the coagulation rate is drastically increased by a small increase of the space scale or the mean fluctuating velocity for the case where the discharge flow from the impeller is negligible, while the overall coagulation rate does not depend as conspicuously on the space scale or the fluctuating velocity for the case where turbulent energy is propagated by the discharge flow. Thus the flow structure around the impeller strongly affects the process performance. It may, however, be difficult to control the space scale and the fluctuating velocity of turbulence separately in the vicinity of the impeller.

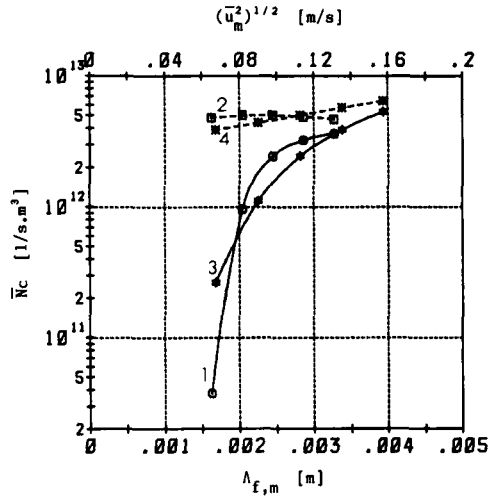


FIG. 17. Effect of the structure of turbulence determined by the impeller-baffle plate system on the overall coagulation rate of monodispersed particles. Solid lines correspond to turbulent diffusion only, while broken lines correspond to turbulent diffusion with convection. $z_0 = 0.15$ m, $n = 3\ s^{-1}$, $d = 0.15$ m. (1) and (2): Relationship between the space scale and the coagulation rate. (3) and (4): Relationship between the mean fluctuating velocity and the coagulation rate.



Consequently, the mixing performance can be easily evaluated under any operating conditions by a numerical analysis that takes into account the decay process of turbulent energy in the stirred vessel. Therefore, the optimum design and the scale-up formulation will be facilitated. Although the coagulation process has been discussed as a mass transfer model, similar numerical simulations are possible for other mass transfer processes by incorporating the process dynamics into the turbulent diffusive processes.

## CONCLUSION

A microhydrodynamic approach to optimum design and formulation of a scale-up rule for a stirred vessel has been proposed. It has been confirmed that turbulent energy is propagated by diffusive mixing in the stirred vessel. The energy spectrum function has been derived from the longitudinal velocity correlation function. Then the decay process of tur-

bulent energy has been deduced from the energy spectrum function by supposing isotropic turbulence in any spaces in the vessel. The stochastic mean of the fluctuating velocities, the integral space scale, and the energy dissipation rate have been correlated with operating variables of the stirred vessel such as the diameters of the vessel and the impeller, the rotational speed of the impeller, etc. The particle behavior in the stirred vessel has been described by a turbulent diffusion equation with the space variant diffusion coefficient. It has been reasonably assumed that the turbulent diffusion coefficient for a fine solid particle is identical with that for a fluid element surrounding the particle. The turbulent coagulation process has been accepted as a model of mass transfer processes in the stirred vessels. Then the coagulation performance has been numerically evaluated in relation to operating variables such as the diameter and the rotational speed of the impeller, the location of a single impeller or multiple impellers, and the impeller-baffle plate structure. These approaches may be more versatile than conventional approaches for optimum design and formulation of the scale-up rule, and any process dynamics can be easily incorporated in the turbulent diffusive processes. Moreover, the mixing performance can be easily evaluated by numerical analysis not only on an overall basis but also as a local aspect of the process behavior.



## SYMBOLS

| | |
|---|---|
| $A$ | value given by Eq. (37) ($s^{-1}$) |
| $a_1$, $a_2$, $a_3$ | proportional constants involved in Eqs. (29), (32), and (30), respectively (-) |
| $B$ | value given by Eq. (38) (-) |
| $C$ | solids concentration on count basis ($m^{-3}$) |
| $D$ | diameter of the cylindrical stirred vessel (m) |
| $d$ | diameter of the impeller (m) |
| $D_t$ | turbulent diffusion coefficient ($m^2/s$) |
| $D_t'$ | turbulent diffusion coefficient of a solid particle ($m^2/s$) |
| $d_p$ | particle diameter (m) |
| $E(\kappa,t)$ | energy spectrum function ($m^3/s^2$) |
| $f(r,t)$ | longitudinal velocity correlation function (-) |
| $H$ | height of the cylindrical stirred vessel (m) |
| $K$ | coefficient involved in Eq. (39) (-) |
| $L$ | transport length (m) |

| | |
|---|---|
| $n$ | rotational speed of the impeller ($s^{-1}$) |
| $N_c$ | coagulation rate on count basis ($s^{-1}$) |
| $N_f$ | flow number (-) |
| $N_{Re}$ | Reynolds number (-) |
| $Q$ | volume flow rate of the discharge flow ($m^3/s$) |
| $r$ | spatial length (m) |
| $R_E(\tau)$ | Eulerian time correlation function (-) |
| Su | spectrum density function ($m^2/s$) |
| $t$ | time coordinate |
| $T(\kappa,t)$ | energy transfer function ($m^3/s^3$) |
| $t_0$ | characteristic time defined by Eq. (21) |
| $U$ | mean velocity (m/s) |
| $u$ | fluctuating velocity (m/s) |
| $v$ | particle velocity in the axial direction (m/s) |
| $w$ | discharge flow velocity (m/s) |
| $w_0$ | discharge flow velocity observed in the vicinity of the impeller (m/s) |
| $x$ | space coordinate |
| $z$ | axial space coordinate |



## Greek

| | |
|---|---|
| $\alpha$ | coefficient involved in Eq. (23) (-) |
| $\beta$ | coefficient involved in Eq. (39) (-) |
| $\gamma$ | proportional constant involved in Eq. (15) ($m^7/s^2$) |
| $\varepsilon$ | energy dissipation rate ($m^2/s^3$) |
| $\eta$ | coefficient involved in Eq. (34) (-) |
| $\kappa$ | wavenumber ($m^{-1}$) |
| $\Lambda_f$ | integral space scale of turbulence (m) |
| $\lambda_0$ | Kolmogorov's microscale (m) |
| $\mu$ | viscosity (Pa · s) |
| $\nu$ | kinematic viscosity ($m^2/s$) |
| $\rho$ | density ($kg/m^3$) |
| $\tau$ | time increment (s) |
| $T_E$ | integral time scale of turbulence (s) |
| $\omega$ | frequency ($s^{-1}$) |

## Subscripts

| | |
|---|---|
| $f$ | fluid |
| $m$ | observed |
| $p$ | particle |

## Superscript

| | |
|---|---|
| $-$ | average |



## REFERENCES


1. V. W. Uhl and J. B. Gray, *Mixing, Theory and Practice,* Vols. 1 and 2, Academic, New York, 1966 and 1967.
2. S. Nagata, *Mixing, Principle and Applications,* Kodansha, Tokyo, 1975.
3. H. Voit and A. Mersmann, *Ger. Chem. Eng., 9,* 101 (1986).
4. F. L. D. Cloete and M. C. Coetzee, *Powder Technol., 46,* 239 (1986).
5. A. H. P. Skelland and G. G. Ramsay, *Ind. Eng. Chem. Res., 26,* 77 (1987).
6. R. S. Brodkey (ed.), *Turbulence in Mixing Operations,* Academic, New York, 1975.
7. E. M. Uram and V. W. Goldschmidt (eds.), in *Fluid Mechanics of Mixing,* ASME, New York, 1973.
8. J. Y. Oldshue, in *Papers of the World Congress III of Chemical Engineering,* Tokyo, 1986, 8k-251.
9. A. B. Mersmann, in *Papers of the World Congress III of Chemical Engineering,* Tokyo, 1986, 8k-254.
10. H. D. Laufhutte and A. Mersmann, *Vortrag auf dem Jahrestreffen 1985 der Verfahrensingenieure in Hamburg,* 1985.
11. J. O. Hinze, *Turbulence,* 2nd ed., McGraw-Hill, New York, 1975.
12. M. Nonaka and T. Uchio, *Sep. Sci. Technol., 19,* 337 (1984).
13. M. Nonaka, T. Inoue, and T. Imaizumi, in *Papers of the 14th International Mineral Processing Congress,* Toronto, 1982, III-9.
14. M. Nonaka, "Study of the Hydrodynamic Characteristics of Flotation Machines," Dissertation, 1981.
15. V. G. Levich, *Physicochemical Hydrodynamics,* Prentice-Hall, Englewood Cliffs, New Jersey, 1962.


*Received by editor July 20, 1989*